Radiative heat transfer at the nanoscale

Author: Alex Reyner Viñolas
*Facultat de Física, Universitat de Barcelona, Diagonal 645, 08028 Barcelona, Spain.**

Advisor: Ivan Latella

Abstract: Macroscopic objects at thermal equilibrium emit electromagnetic radiation which is in equilibrium with the objects. If two bodies have different temperatures, they can exchange heat without contact by means of the emitted thermal radiation. For separations large enough between the bodies, the power exchanged is described by the well-known Stefan-Boltzmann law and is bounded by the backbody limit. But, what happens when the gap between the two of them is reduced to much smaller distances? At the nanoscale, the blackbody limit law can be exceeded by several orders of magnitude due to the contribution of evanescent waves standing close to the surfaces of the bodies. In this TFG, we study this phenomenon at a theoretical level and numerically calculate the heat flux between to semi-infinite bodies considering concrete materials such as silicon carbide and gold.

I. INTRODUCTION

Due to thermal excitation of charges within material media, all bodies emit electromagnetic waves carrying energy. The total energy radiated per unit surface area and time for an ideal blackbody is given by the Stefan-Boltzmann law. Moreover, if two of these blackbodies are considered at different temperatures T_1 and T_2, the net energy flux exchanged by the objects is given by

$$\Phi_{\mathrm{BB}} = \sigma \left(T_1^4 - T_2^4\right), \tag{1}$$

where σ is the Stefan-Boltzmann constant.

The microscopic details of blackbody radiation were successfully described by Planck with his theory of heat radiation [1], in turn giving rise to the first quantum theory. An important assumption in Planck's theory is that the dimensions of the system are large as compared with the length scale specified by the inverse of the typical wavenumber of the radiation. A characteristic length defining this scale at temperature T can be written as $\lambda_T = \hbar c/k_B T$, where c is the speed of light in vacuum, $\hbar$ is the reduced Planck constant and k_B is the Boltzmann constant. In particular, surface effects are completely neglected in this theory and expression (1) for the radiative heat transfer does not depend on the separation distance between the bodies which is accordingly assumed much larger than λ_T. At room temperature we have $\lambda_T \approx 8\,\mu$m, so radiative energy fluxes are expected to be modified when the separation between the objects is reduced down to the nanoscale.

Surface effects play a mayor role in nanoscale radiative heat transfer [2]. In order to describe such surface effects, let us consider light waves of frequency ω crossing a planar interface on the x-y plane. Suppose that the interface separates one medium (body 1) from vacuum. The component of the wavevector perpendicular to the interface in the vacuum region is given by $k_z = \sqrt{\omega^2/c^2 - k^2}$, where $k^2 = k_x^2 + k_y^2$ is the parallel wavevector component. Waves with $k > \omega/c$ present total internal reflection, corresponding to an incident angle θ greater than the critical angle θ_C, since the parallel component is conserved across the interface and k_z becomes imaginary. These large values of k lead to evanescent modes that decay exponentially with the distance from the interface, and do not really contribute to energy emission when a single interface is considered. This is very important, since, un-

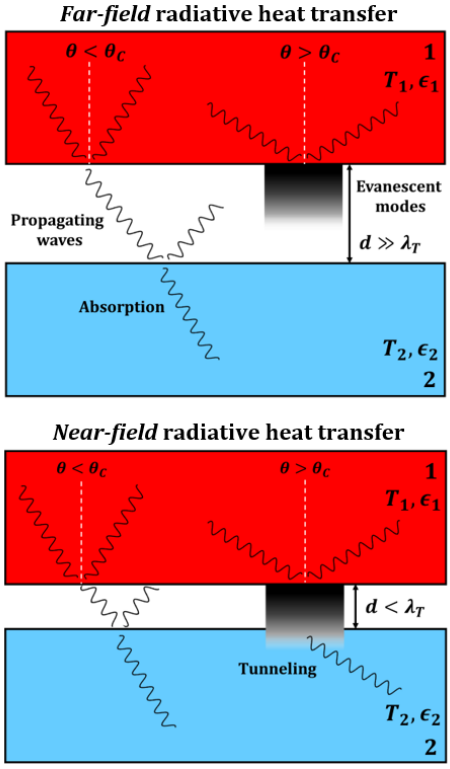

FIG. 1: Illustration of the two different regimes of radiative heat transfer and schematic representation of the system

*Electronic address: areynerv@gmail.com

der these conditions, the total energy flux emitted into vacuum can not exceed that calculated via the Stefan-Boltzmann law (which neglects surface effects). We consider now that a second interface separating the vacuum region from a second medium (body 2) is placed at a distance d from the first interface. If d is large enough such that evanescent modes are suppressed in the vacuum gap, namely, at $d \gg \lambda_T$, only the usual propagating modes contribute to energy transfer and expression (1) applies for blackbodies. This corresponds to the so-called far-field regime of radiative heat transfer. In contrast, when $d < \lambda_T$, the total internal reflection is "frustrated" and evanescent waves originating at one of the interfaces can cross the vacuum gap reaching the other interface. In this case, evanescent waves contribute to energy transport as well, which corresponds to the near-field regime of radiative heat transfer. This energy transport mechanism is also known as *photon tunneling* [3] and can be the dominant contribution to radiative heat exchange at the nanoscale [5–9]. An illustration of the two different regimes of radiative heat transfer is shown in Fig. 1.

In this TFG, we study the radiative heat transfer between two bodies separated by nanoscale vacuum gaps by considering concrete materials and the corresponding comparison with the ideal backbody case. The rest of this work is organized as follows. In Sec. II we describe the theory accounting for the radiative heat transfer in near-field regime and the expressions we are going to use after. In Sec. III we consider some numerical results. In Sec. IV we consider a theoretical limit and, finally, in Sec. V we present our concluding remarks.

II. RADIATIVE HEAT TRANSFER FROM FLUCTUATIONAL ELECTRODYNAMICS

The energy per unit surface and unit time carried by electromagnetic waves is given by the Pointing vector $\mathbf{S}(\mathbf{r},t) = \mathbf{E}(\mathbf{r},t) \times \mathbf{H}(\mathbf{r},t)$, where $\mathbf{E}$ and $\mathbf{H}$ are the electric and magnetic fields at a point $\mathbf{r}$ in space and time t. In the geometry of our system, the radiative heat flux Φ is given by the average component of the Poynting vector in the direction perpendicular to the surfaces of the bodies, so that $\Phi = \langle S_z(\mathbf{r},t)\rangle$, where $\langle\cdots\rangle$ indicates statistical average. Furthermore, within the framework fluctuational electrodynamics, one assumes that the thermal radiation is generated by fluctuating electric currents $\mathbf{J}$ inside the bodies [2]. These currents act as stochastic sources in Maxwell equations which in the frequency domain take the form

$$\boldsymbol{\nabla} \times \mathbf{E}(\mathbf{r},\omega) = i\omega\mu_0 \mathbf{H}(\mathbf{r},\omega), \tag{2}$$

$$\boldsymbol{\nabla} \times \mathbf{H}(\mathbf{r},\omega) = -i\omega\varepsilon_0\varepsilon(\omega)\mathbf{E}(\mathbf{r},\omega) + \mathbf{J}(\mathbf{r},\omega), \tag{3}$$

where μ_0 and ε_0 are the vacuum permeability and permittivity, respectively, and $\varepsilon(\omega)$ is the relative permittivity of the considered body. The fluctuating current densities inside the bodies vanish in average, $\langle \mathbf{J} \rangle = 0$, but their correlations are finite and given by the fluctuation-dissipation theorem [2, 5]

$$\langle J_a(\mathbf{r},\omega) J_b^*(\mathbf{r}',\omega')\rangle = \frac{4\hbar\omega^2\varepsilon_0}{\pi}\mathrm{Im}[\varepsilon(\omega)]n(\omega,T) \times \delta_{ab}\delta(\mathbf{r}-\mathbf{r}')\delta(\omega-\omega'), \tag{4}$$

where $a, b = x, y, z$ and $n(\omega,T) = \left[e^{\hbar\omega/k_BT} - 1\right]^{-1}$ is the Bose-Einstein distribution at temperature T. Thus, Maxwell equations can be solved using (4) and the mean energy flux in the vacuum gap can be computed.

As a result, the radiative heat flux can be written as

$$\Phi(d) = \int_0^\infty \frac{d\omega}{2\pi}\varphi(\omega,d), \tag{5}$$

with the spectral flux given by

$$\varphi(\omega,d) = \hbar\omega n_{1,2}(\omega)\int_0^\infty \frac{dk}{2\pi}k\sum_p \mathcal{T}_p(\omega,k,d), \tag{6}$$

where $\mathcal{T}_p(\omega,k,d)$ are the energy transmission coefficients for polarizations $p = \mathrm{TE}, \mathrm{TM}$. We have introduced the notation $n_{1,2}(\omega) = n(\omega,T_1) - n(\omega,T_2)$, where T_1 and T_2 are the temperatures of bodies 1 and 2, respectively.

The energy transmission coefficients account for both propagating ($k < \omega/c$) and evanescent waves ($k > \omega/c$), explicitly given by

$$\mathcal{T}_p(\omega,k,d) = \begin{cases} \frac{\left(1-|r_p^1|^2\right)\left(1-|r_p^2|^2\right)}{\left|1-r_p^1 r_p^2 e^{i2k_z d}\right|^2} & k < \omega/c \\ \frac{4\,\mathrm{Im}\left(r_p^1\right)\mathrm{Im}\left(r_p^2\right)e^{-2\,\mathrm{Im}(k_z)d}}{\left|1-r_p^1 r_p^2 e^{-2\,\mathrm{Im}(k_z)d}\right|^2} & k > \omega/c \end{cases} \tag{7}$$

r_p^j are the Fresnel reflection coefficients for body $j = 1, 2$,

$$r_{\mathrm{TE}}^j = \frac{k_z - k_{zj}}{k_z + k_{zj}} \quad \text{and} \quad r_{\mathrm{TM}}^j = \frac{\varepsilon_j k_z - k_{zj}}{\varepsilon_j k_z + k_{zj}}, \tag{8}$$

for which

$$k_{zj} = \sqrt{\frac{\omega^2}{c^2}\varepsilon_j(\omega) - k^2} \tag{9}$$

is the z-component of the wavevector in medium j characterized by its permittivity $\varepsilon_j(\omega)$.

III. CONCRETE EXAMPLES

As examples of application, we consider the heat transfer between bodies 1 and 2 assumed to be made of specific materials such as silicon carbide (SiC) and gold (Au), corresponding to a polar material and a metal respectively. The permittivity of SiC is given by the Drude-Lorentz model [10]

$$\varepsilon(\omega) = \varepsilon_\infty \frac{\omega_L^2 - \omega^2 - i\Gamma\omega}{\omega_T^2 - \omega^2 - i\Gamma\omega}, \tag{10}$$

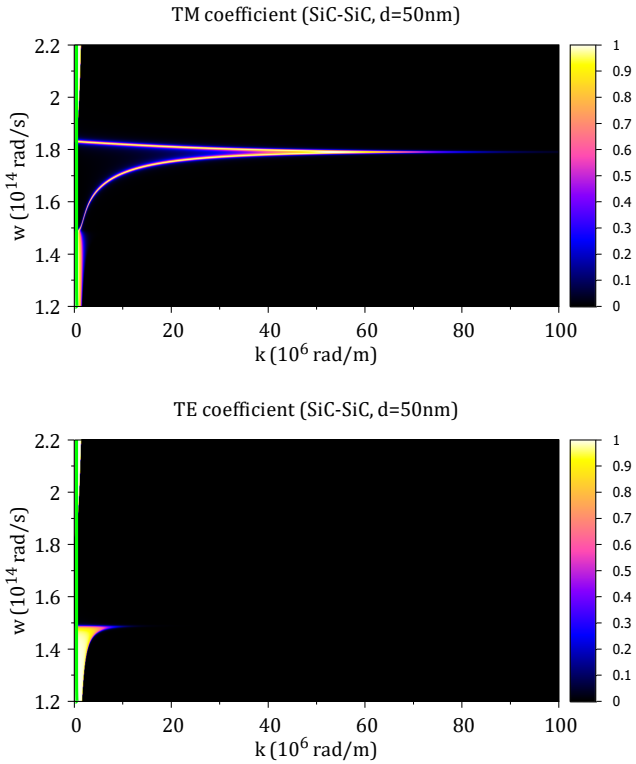

FIG. 2: Energy transmission coefficients $\mathcal{T}_p$ for TM and TE polarizations in the case of SiC at $d = 50\,\text{nm}$. In green we show the light line where $k = \omega/c$.

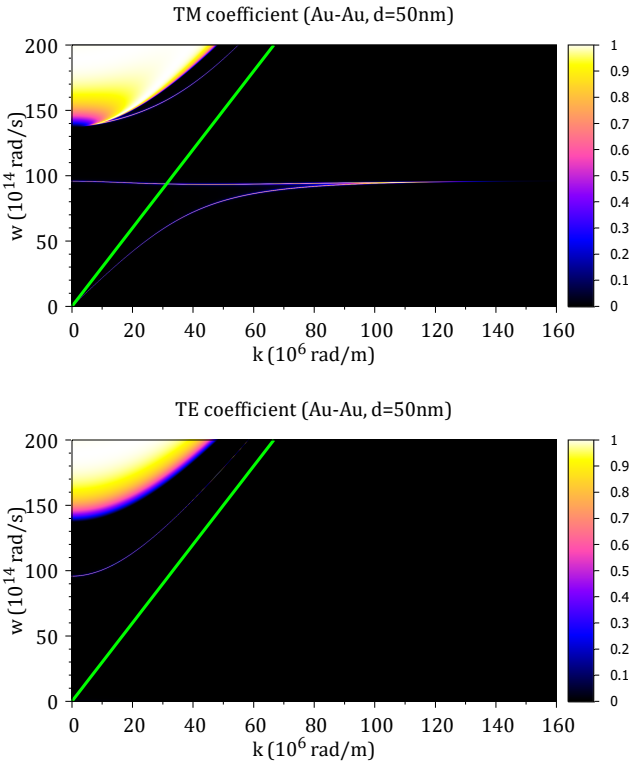

FIG. 3: Energy transmission coefficients $\mathcal{T}_p$ for TM and TE polarizations in the case of Au at $d = 50\,\text{nm}$. In green we show the light line where $k = \omega/c$.

with infinite-frequency dielectric constant $\varepsilon_\infty = 6.7$, longitudinal optical frequency $\omega_L = 1.83 \times 10^{14}\,\text{rad/s}$, transverse optical frequency $\omega_T = 1.49 \times 10^{14}\,\text{rad/s}$, and damping $\Gamma = 8.97 \times 10^{11}\,\text{rad/s}$. For Au we consider the Drude model [11]

$$\varepsilon(\omega) = 1 - \frac{\omega_P^2}{\omega(\omega + i\Gamma)}, \tag{11}$$

with plasma frequency $\omega_P = 1.37 \times 10^{16}\,\text{rad/s}$ and dissipation rate $\Gamma = 5.32 \times 10^{13}\,\text{rad/s}$.

Now, we have all ingredients to calculate the radiative heat transfer between two bodies as a function of the separation d. To do it, I made a `Fortran` program to integrate equations (5) and (6), and another that returns the values of the energy transmission coefficients (7) for given ω, k and d. All the simulations have been done with the same temperatures: $T_1 = 400\,\text{K}$ for body 1 and $T_2 = 300\,\text{K}$ for body 2.

A. Energy transmission coefficients

Firstly, as all the code is build around them, we need to discuss our results on the transmission coefficients. We have decided to use $d = 50\,\text{nm}$ as a representative example in which the heat transfer takes place in near-field regime. In Fig. 2 and Fig. 3, it can be seen that there are resonances inside the material. The resonance is characteristic of each material and can be excited at small separations where evanescent modes are active. For SiC the two resonances in the TM coefficient converge into a single line that vanishes at large values of k. This is called the *surface-phonon polariton* and arises as a coupling of an optical phonon with the electromagnetic field in polar materials. The frequency of the polariton depends on the material and its structure. As we will see later on, this polariton is the main contributor to the radiative heat transfer at small separations.

B. Spectral energy flux

Here we compute the spectral energy flux, from equation (5), focusing on the case of two bodies made of SiC. In the numerical calculation it is not necessary to integrate for $k \to \infty$, since for $k > 10/d$ the contribution of evanescent waves is negligible. For example, using $d = 50\,\text{nm}$ as before, $k_{max} = 200 \times 10^6\,\text{rad/m}$. This value matches with what we can see in Fig. 2.

In Fig. 4, it is clearly seen that for SiC almost all the energy is emitted at a certain frequency. We have a peak at $\omega \approx 1.8 \times 10^{14}\,\text{rad/s}$, which corresponds to the

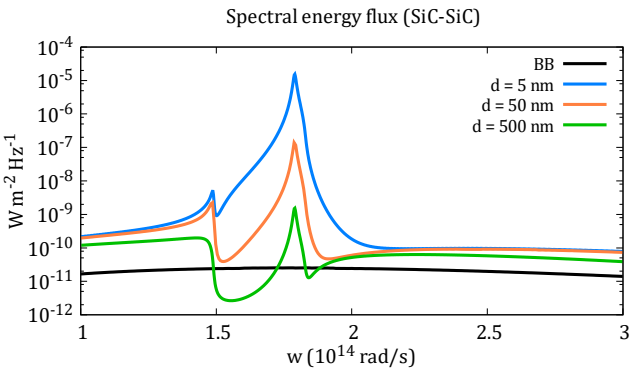

FIG. 4: Spectral energy flux $\varphi(\omega, d)$ for different gap thicknesses d between two SiC bodies at $T_1 = 400\,\mathrm{K}$ and $T_2 = 300\,\mathrm{K}$. The blackbody case is shown in back for comparison.

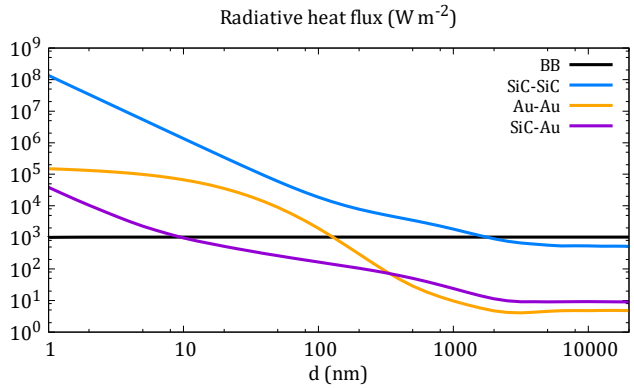

FIG. 5: Radiative heat flux $\Phi(d)$ between two bodies at $T_1 = 400\,\mathrm{K}$ and $T_2 = 300\,\mathrm{K}$ as a function of the separation d. The heat flux between two blackbodies is shown for comparison.

surface-phonon polariton in the TM coefficient. Despite its transmission coefficient having smaller values than for $k < \omega/c$, as seen in Fig. 2, the large number of available modes makes it the dominant contribution to the heat flux [4]. Also, the small peak at $\omega \approx 1.5 \times 10^{14}\,\mathrm{rad/s}$ appears in the TE coefficient, but it fades away quickly. For high ω the Bose-Einstein distribution nullifies any contribution, hence we do not have energy emission at high frequencies. The case of the Au is the perfect example for the importance of the Bose-Einstein distribution. We have a resonance at $\omega \sim 100 \times 10^{14}\,\mathrm{rad/s}$ in the TM coefficient, as seen in Fig. 3, but due to this it does not contribute to the radiative heat transfer.

C. Radiative heat flux

These are the final results of the radiative heat flux for different pairs of surfaces: SiC-SiC, Au-Au and SiC-Au. We also compute the heat exchange for two blackbodies to compare the results, which using the Stefan-Boltzmann law (1) gives $\Phi_{\mathrm{BB}} \simeq 992\ \mathrm{W/m^2}$ at the considered temperatures. This is necessary, as for large distances the computed radiative heat flux should not be larger than the blackbody limit.

As we can see in Fig. 5, the transmission between two SiC surfaces is much better than between two of Au. For SiC we observe that at $d < 100\,\mathrm{nm}$, $\Phi(d) \propto d^{-2}$.This dependence on the separation distance is characteristic of polar materials at small d [4], see the Appendix for a brief explanation. We can show that for Au the same happens for much smaller distances, but it does not have any interest for the problem we are studying.

It is interesting to note that the photon tunneling starts to be significant at $d \sim 6\,\mu\mathrm{m}$, that is approximately the value of λ_T obtained at $T = 400\,\mathrm{K}$. We also highlight that the present theory makes no sense for separation distances comparable to the typical size of the atoms. That is why we have not worked at separations smaller than the nanometer.

IV. STEFAN-BOLTZMANN LAW AS A LIMITING CASE

At the macroscopic scale, we know that the energy emitted by a body at temperature T can never surpass the one for an ideal blackbody at that temperature. In order to consider a blackbody in the present theory, one can set the Fresnel reflection coefficients (8) to zero. In this case $\mathcal{T}_p = 1$ for $k < \omega/c$ and zero otherwise. Using this and computing the integral over k in (6) we obtain Planck's law:

$$\varphi(\omega) = \frac{\hbar\omega^3}{4\pi^2 c^2}\left(\left[e^{\hbar\omega/k_B T_1} - 1\right]^{-1} - \left[e^{\hbar\omega/k_B T_2} - 1\right]^{-1}\right).$$

The integral over frequencies of the expression above leads to the Stefan-Boltzmann law. For real materials, in general, the Fresnel reflection coefficients are not equal to 0, as in our case. This makes $\mathcal{T}_p < 1$ and the result obtained for the heat exchange in far-field regime are below the backbody limit, as can be observed in Fig. 5.

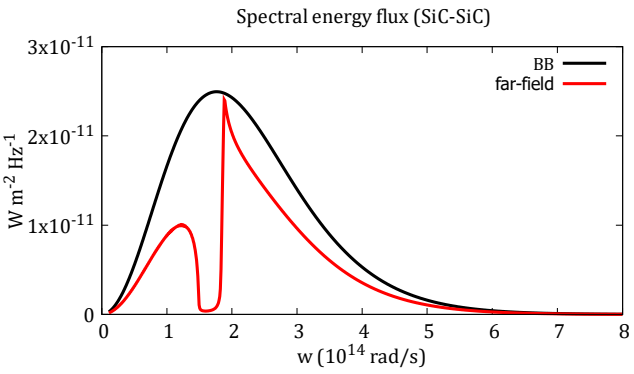

FIG. 6: Comparison between the spectral energy flux of an ideal blackbody and the one calculated for the SiC in far-field regime, at $d = 500\,\mu\mathrm{m}$. This figure can also be compared with Fig. 4.

Regarding the spectral emission, as can be seen in Fig. 6, we note that the surface-phonon polariton no longer contributes to the heat exchange when it takes place in far-field regime. This is in agreement with the theory, as for the far field the evanescent modes disappear. The region where the spectral energy flux is close to 0 is called the *reststrahlen band*. The *reststrahlen effect* is a reflectance phenomenon in which energy for a narrow band can not propagate in the medium due to changes in the reflective coefficients. The incident radiation to that medium experiences strong reflection.

In addition, another thing we must keep in mind is the computational power. To obtain better results we should use more integration points or more precise integration methods. Doing so should not change the results, but little corrections and smoothness.

V. CONCLUSIONS

To summarize, we have verified that the transferred heat between two surfaces through a vacuum increases when the gap between them is small enough. In fact, the radiative heat transfer at nanoscale is several times bigger than the classic transfer given by Planck's equation and the blackbody law. Opposed to this last one, the radiative heat flux in the near-field highly depend on the distance. At not relatively high temperatures, this starts to show when we are below some micrometers. We have observed that most of the heat transfer is due to specific resonances in the material that propagate through the evanescent modes. So, the heat transfer presents emission peaks for some frequencies making it almost monochromatic. Finally, as the theory predicts, we have obtained that this evanescent modes vanish in the far field.

This effect can have several applications. One that has been studied lately is related to thermophotovoltaics and energy conversion. Photovoltaic (PV) cells have a certain range of wavelenght where they work better, as photons with energies below the semiconductor band gap do not generate electricity and photons with larger energies loose part of the energy thermally. Typically, the temperature of the hot emitter is too low to have a sufficient photon flux to the PV cell. However near-field radiative heat transfer may increase the photon flux and power output. The technical challenges of reaching and maintaining high temperature differences and nanoscale gaps make this impossible on a large scale at the moment. For the time being, microscale devices that demonstrate this effect have been experimentally realized [12].

Appendix: Quasistatic limit

Here we want to show that at small enough separations the heat exchange scales as $1/d^2$. This can be shown by considering the quasistatic limit for which $k \gg \omega/c$. We then have $k_z \simeq ik$ and the Fresnel coefficients asymptotically become [5]

$$\lim_{k\to\infty} r_{\mathrm{TE}} = \frac{\varepsilon(\omega)-1}{4c^2k^2/\omega^2} \qquad \lim_{k\to\infty} r_{\mathrm{TM}} = \frac{\varepsilon(\omega)-1}{\varepsilon(\omega)+1}. \quad \text{(A.1)}$$

Thus, r_{TE} vanishes and r_{TM} does not depend on k. Taking this into account and considering only the contribution of evanescent modes in the spectral flux, we get

$$\varphi(\omega,d) \propto \mathrm{Im}\int_0^\infty \frac{dk}{2\pi}\frac{kr_{\mathrm{TM}}^2 e^{-2kd}}{1-r_{\mathrm{TM}}^2 e^{-2kd}} \propto \frac{1}{d^2}. \quad \text{(A.2)}$$

This behaviour can be observed in Fig. 5 for SiC, which, as previously noted, is a polar material. For metals such as Au, the $1/d^2$ scaling regime typically occurs at separations much smaller than the nanometer.

Acknowledgments

Firstly, I'd like to deeply thank professor Ivan. This project would not have been possible without his advice, guidance and help.

I also want to mention my parents and sister, that listened to me nearly every day and motivated me to do a better job. And not less important, my colleagues for the support all this last year.

[1] M. Planck, *The theory of heat radiation* (P. Blakiston's Son & Co., 1914).
[2] D. Polder and M. van Hove, *Phys. Rev. B 4, 3303* (1971).
[3] J. B. Pendry, *J. Phys.: Condens. Matter 11, 6621* (1999).
[4] J.-P. Mulet, K. Joulain, R. Carminati & J.-J. Greffet, *Enhanced Radiative Heat Transfer at Nanometric Distances, Microscale Thermophysical Engineering, 6:3, 209-222* (2002).
[5] K. Joulain, J.-P. Mulet, F. Marquier, R. Carminati, and J.-J. Greffet, *Surf. Sci. Rep. 57, 59-112* (2005).
[6] S.-A.Biehs, E. Rousseau and J.-J. Greffet, *Phys. Rev. Lett. 105, 234301* (2010).
[7] I. Latella, et al., *Phy. Rev. B 95, 205404* (2017).
[8] J. C. Cuevas and F. J. García-Vidal, *Radiative Heat Transfer. ACS Photonics 2018, 5, 3896-3915* (2018).
[9] S.-A. Biehs, et al., *Rev. Mod. Phys, 93* (2021).
[10] *Handbook of Optical Constants of Solids*, edited by E. Palik (Academic Press, New York, 1998).
[11] M. A. Ordal, Robert J. Bell, R. W. Alexander, L. L. Long, and M. R. Querry, *Appl. Opt. 24, 4493* (1985).
[12] A. Fiorino, et al., *Nanogap near-field thermophotovoltaics. Nature Nanotech 13, 806–811* (2018).
[13] B. Juliá and M. Ibañes, *Física Computacional* (2021).